Unusual long-range spin-spin coupling in fluorinated polyenes: A mechanistic analysis

Jürgen Gräfenstein[a)]
Department of Chemistry, Göteborg University, S-41296 Göteborg, Sweden

Dieter Cremer
Department of Chemistry, University of the Pacific, 3601 Pacific Ave., Stockton, California 95211-0110, USA
and Department of Physics, University of the Pacific, 3601 Pacific Ave., Stockton, California 95211-0110, USA

(Received 13 June 2007; accepted 28 August 2007; published online 5 November 2007)

Nuclear magnetic resonance (NMR) is a prospective means to realize quantum computers. The performance of a NMR quantum computer depends sensitively on the properties of the NMR-active molecule used, where one requirement is a large indirect spin-spin coupling over large distances. F–F spin-spin coupling constants (SSCCs) for fluorinated polyenes $F-(CH{=}CH)_n-F$ $(n=1\cdots5)$ are >9 Hz across distances of more than 10 Å. Analysis of the F,F spin-spin coupling mechanism with our recently developed decomposition of *J* into Orbital Contributions with the help of Orbital Currents and Partial Spin Polarization (J-OCOC-PSP=J-**OC**-PSP) method reveals that coupling is dominated by the spin-dipole (SD) term due to an interplay between the π lone-pair orbitals at the F atoms and the $\pi(C_{2n})$ electron system. From our investigations we conclude that SD-dominated SSCCs should occur commonly in molecules with a contiguous π-electron system between the two coupling nuclei and that a large SD coupling generally is the most prospective way to provide large long-range spin-spin coupling. Our results give guidelines for the design of suitable active molecules for NMR quantum computers. © *2007 American Institute of Physics*. [DOI: 10.1063/1.2787001]

I. INTRODUCTION

Nuclear magnetic resonance (NMR) spectroscopy has developed during a period of more than 50 years as one of the most important tools for structure elucidation.[1–5] In the last ten years, NMR has become attractive for a quite different field of applications, viz, the construction of quantum computers,[6] which would allow us to solve problems of a complexity inaccessible to classical computers. A NMR-based quantum computer takes advantage of the spin states of the nuclei of a suitable NMR-active substance. The spin states are used to encode qubits (quantum bits), by which the calculations of a quantum computer are performed.[7,8] The NMR properties of the chemical compound used in this connection are crucial for the performance of the quantum computer. Mawhinney and Schreckenbach[9] have specified the requirements for an appropriate NMR-active molecule to be used for quantum computing: (i) the molecule should contain as many NMR-active nuclei as possible; (ii) it should possess different chemical shifts for each active nucleus; (iii) also needed is a contiguous network of sizable spin-spin coupling constants (SSCCs) *J* between the active nuclei. Requirement (i) implies that the molecules in question should be relatively large. In view of (i) and (iii), molecules with sizable SSCCs across a large number of bonds and large geometrical distances are interesting candidates for large SSCCs. Indirect nuclear spin-spin coupling in saturated systems is typically short ranged and measurable SSCCs across four or more bonds occur only in exceptional cases (see, e.g., Refs. 10 and 11). In extended unsaturated molecules, in contrast, the delocalized π-electron system can provide long-range spin-spin coupling,[12] and measurable SSCCs over nine bonds have, e.g., been observed in polyyne derivatives.[13] In an investigation of the indirect spin-spin coupling in polyenes[14] we predicted observable SSCCs between H atoms across 15 and more bonds. Another example for far-reaching SSCCs are F,F couplings. For instance, $^5J(F,F)$ was measured to be 35.7 Hz in 1,1,4,4-tetrafluoro-1,3-butadiene,[15(a)] 17.5 Hz in *p*-difluorobenzene,[15(b)] and 39 Hz in 1,4-difluorocubane.[15(c)]

By combining the observations made for polyenes and difluorosubstituted hydrocarbons, one should expect large long-range coupling in unsaturated hydrocarbons (e.g., polyenes) where the coupling nuclei are substituted by fluorine. Provasi *et al.*[16] have recently calculated long-range F,F-SSCCs in fluorinated polyenes, cumulenes, and polyynes by the second-order polarization propagator approximation (SOPPA).[17,18] In agreement with available experimental data,[15,19] the calculations in Ref. 16 predict F,F-SSCCs considerably larger than the corresponding H,H-SSCCs in unsubstituted polyenes,[12,14] with F,F-SSCCs of ⩾9 Hz being predicted across 11 bonds and a geometric distance of more than 11 Å. Apart from their extraordinary size, the F,F-SSCCs in these molecules are unusual in other regards: Indirect spin-spin coupling is typically dominated by the

[a)]Electronic mail: jurgen.grafenstein@chem.gu.se

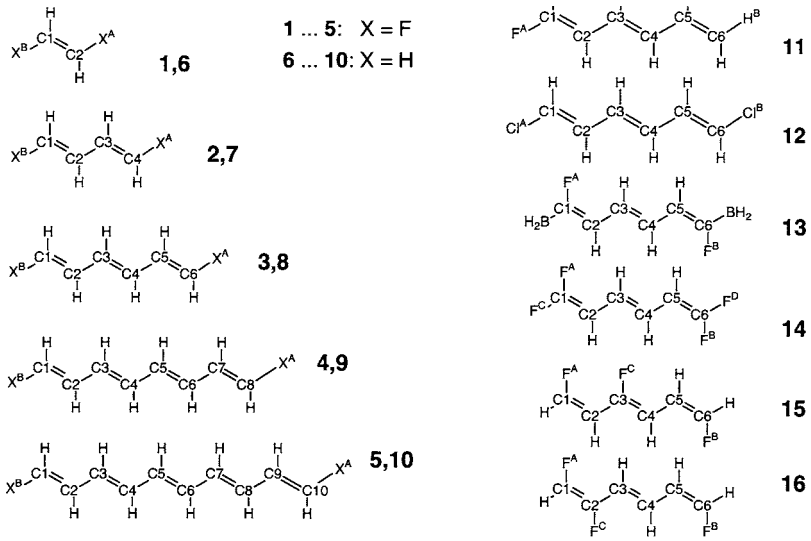

SCHEME 1. Structures of the compounds investigated in this work and atom numbering.

Fermi-contact (FC) coupling mechanism,[20] which is the case, e.g., for the long-range H,H coupling in polyenes.[14] The long-range F,F coupling mechanism, in contrast, is dominated by paramagnetic spin-orbit (PSO) coupling[20] for polyynes and cumulenes and by spin-dipole (SD) coupling[20] for polyenes. This is in line with earlier theoretical investigations for fluorinated unsaturated hydrocarbons by Peruchena *et al.*[21] and with recent findings stating that the PSO and SD terms in F,F-SSCCs are often sizable or even dominant.[22,23] The SD dominance is noteworthy because the SD term was often considered negligible in previous calculations and has been ignored in early implementations for the calculation of SSCCs,[24] as well as in many investigations of F,F-SSCCs (see, e.g., Ref. 25).

The fluorinated hydrocarbons investigated by Provasi *et al.*[16] fulfill requirement (iii) of Mawhinney and Schreckenbach, however, not requirements (i) and (ii), i.e., modifications of these molecules are required to obtain suitable qubit molecules for a NMR-based quantum computer. As a guideline for such modifications, it is essential to identify those features in the coupling mechanism of the fluorinated hydrocarbons that account for the unusually long-ranging F,F coupling. This requires a detailed analysis of the spin-spin coupling mechanism in difluorosubstituted hydrocarbons.

We have recently developed the decomposition of J into orbital contributions with the help of orbital currents and partial spin polarization method (J-**OC**-PSP)[26–28] (see Ref. 29 for a recent review), which makes it possible to decompose the total SSCC into contributions from individual orbitals or orbital groups and detects in this way the most important orbital contributions to the spin-spin coupling mechanism. The analysis is complemented by plotting local quantities such as first-order orbitals as well as magnetization or current densities.[26,27] We will use the J-**OC**-PSP method to elucidate the mechanism responsible for long-range F,F coupling. In this connection we will focus on polyenes for two reasons: first, the SD dominance in the F,F coupling mechanism has to be clarified; secondly, the presence of nonterminal H atoms make the polyenes more flexible for modifications and substitutions needed for designing optimal qubit molecules. Cumulenes and polyynes are less suited in this respect apart from their high reactivity, which hinders in general their application for quantum computing purposes. We will investigate the fluorinated polyenes 1,2-*trans*-difluoroethene **1**, 1,4-all-*trans*-difluoro-1,3-butadiene **2**, 1,6-all-*trans*-difluoro-1,3,5-hexatriene **3**, 1,8-all-*trans*-difluoro-1,3,5,7-octatetraene **4**, and 1,10-all-*trans*- difluoro-1,3,5,7,9-decapentaene **5** (Scheme 1). As suitable reference molecules, we will use ethene **6**, *trans*-butadiene **7**, all-*trans*-hexatriene **8**, all-*trans*-octatetraene **9**, and all-*trans*-decapentaene **10**, which we studied previously.[11,14]

This work will focus on the question how the F substitution in **6–10** yielding **1–5** changes long-range spin-spin coupling, especially its SD contribution. In this connection, we will address the following questions:

(1) Why are the SSCCs $J(\mathrm{F,F})$ for **1–5** dominated by the SD term, whereas the PSO term dominates $J(\mathrm{F,F})$ in fluorinated cumulenes and polyynes?[16]
(2) Does the F substitution provide a sizable "through-tail" coupling between the lone-pair orbitals at the F atoms, similar to the through-tail interaction that accounts for the conformation-dependent $^3J(\mathrm{H,H})$ values in ethane?[11,30]
(3) How does F substitution influence spin-information transfer between the coupling nuclei and the $\pi(\mathrm{C}_{2n})$ ($2n$: number of C atoms in the polyene) system? Which differences exist between FC and SD mechanisms?
(4) Does F substitution make the spin-information transport inside the $\pi(\mathrm{C}_{2n})$ system more efficient compared to the mechanism in **6–10**?[11,14]
(5) Does spin-information transport inside the $\pi(\mathrm{C}_{2n})$ system work more efficiently for the SD mechanism than for the FC mechanism?
(6) Which specific properties of the F atom (small radius, high electronegativity, etc.) are crucial for the large F,F spin-spin coupling?
(7) Is the SD dominance in the long-range coupling in **1–5**

special for a restricted class of fluorinated unsaturated hydrocarbons, or can one expect SD-dominated spin-spin coupling in a larger class of molecules?

This article is structured as follows. In Sec. II, the theory of indirect spin-spin coupling and the J-**OC**-PSP method is summarized, and the strategy of the J-**OC**-PSP investigation for **1–5** is outlined. Section III gives the computational details of the calculations performed. In Sec. IV, the results of the calculations are presented, whereas in Secs. V and VI F,F spin-spin coupling is analyzed and the coupling mechanism discussed. The relevance of results for NMR quantum computing is presented in Sec. VII. Technical details of the J-**OC**-PSP analysis for **1–5** are described in the Appendix.

II. THEORY OF NMR SPIN-SPIN COUPLING

The theory of NMR spin-spin coupling was discussed many times in the literature[1–5,20,29] and therefore we mention here just a few essentials of the mechanism needed for the understanding of the J-**OC**-PSP method.

Ramsey theory of indirect spin-spin coupling. The theory of indirect spin-spin coupling for the nonrelativistic case has been worked out by Ramsey[20] who demonstrated that the total SSCC consists of four terms [*Ramsey terms*: FC, SD, PSO, and diamagnetic spin-orbit (DSO) term]. The FC and SD terms result from a partial spin polarization of the electron system, whereas the two spin-orbit (SO) terms are caused by orbital currents induced in the electron system. For the FC mechanism, spin polarization of the electron system is caused by the strongly localized magnetic field inside the first coupling nucleus (perturbing nucleus) and probed by the corresponding field in the second (responding) nucleus. For the SD term, in contrast, partial spin polarization of the electron system is generated and probed by the extended magnetic dipole fields outside the coupling nuclei. One can associate the DSO term with the induced Larmor precession of the electron system and the PSO term with the modification of previously existing electronic ring currents. Strictly speaking, only the total SO term is unambiguous, whereas PSO and DSO terms individually cannot be uniquely defined because of the gauge ambiguity for the vector potential of any magnetic field.[31]

The spin-spin coupling mechanism depends on the orientation of the perturbing nucleus. The SSCC is thus a second-rank tensor, and the experimentally interesting isotropic SSCC is the average of the three diagonal components of this tensor. For the SD mechanism, it is useful to further decompose each of these components into three subcomponents,[32] one for each component of the vector field describing the electronic spin polarization density. We will denote these subcomponents by subscripts (xx), (xy), etc., where, e.g., (xy) refers to the y component of the spin polarization when the perturbing nucleus is oriented in x direction.

*Orbital decomposition of the SSCC: The J-**OC**-PSP method*. The J-**OC**-PSP approach[26–29] specifies which orbitals, alone or in cooperation, are most important for a given SSCC and its Ramsey terms. In the present work, we used J-**OC**-PSP to identify those orbital contributions that account for the long-range coupling in molecules ***1–5***. In a first step, we separated σ and π-electron contributions for $J(\mathrm{F},\mathrm{F})$ in ***1–5*** according to

$$J = J(\sigma) + J(\pi). \tag{1}$$

For this purpose, we calculated the SSCC once with all orbitals active (i.e., in the conventional way), once with all π orbitals frozen. The latter calculation provides $J(\sigma)$, i.e., that part of the SSCC due to the σ electrons alone. The difference of the two SSCC values yields $J(\pi)$, i.e., that part of J that results from the π electrons (alone or in cooperation with the σ electrons). As we are especially interested in the role of the F atoms for long-range coupling, the $J(\pi)$ contribution is analyzed in more detail and decomposed according to

$$J(\pi) = J(\pi(\mathrm{C}_{2n})) + J(\pi(\mathrm{F})) + J(\pi(\mathrm{C}_{2n})) \leftrightarrow \pi(\mathrm{F})) \tag{2}$$

into the contributions of the $\pi(\mathrm{C}_{2n})$ system, the $\pi(\mathrm{F})$ orbitals, and the cooperation between $\pi(\mathrm{C}_{2n})$ system and $\pi(\mathrm{F})$ orbitals, respectively. For $\pi(\mathrm{C}_{2n}) \leftrightarrow \pi(\mathrm{F})$, we will use the shorthand notation $\pi \leftrightarrow \pi$ in the following. The decomposition described in Eqs. (1) and (2) for the total J was performed analogously for each of the Ramsey terms.

Active and passive contributions. In contributions involving more than one orbital, the orbitals may play different roles: One or two of the involved orbitals make an *active* contribution, i.e., interact directly with one or both of the coupling nuclei. The remaining orbitals make a *passive* contribution, i.e., contribute to the spin-information transmission only by interaction with the active (or other passive) orbitals. Only the active orbitals need to obey the selection rules at one or both coupling nuclei.

Passive contributions can be crucial for long-range spin-spin coupling. For instance, the long-range FC coupling in polyenes is provided by the delocalized π electrons despite the fact that the π orbitals, because of their nodal plane, have no contact interaction with the coupling nuclei. Thus, the π electrons can only play a passive role, which implies that active σ orbitals at the coupling nuclei transfer the spin information between the coupling nuclei and the π system.[11,12,14,33,34] For SD and PSO coupling, in contrast, the selection rules do not exclude the π electrons to make an active contribution.

We refined the J-**OC**-PSP analysis for **1–5** by decomposing all π orbital contributions and their Ramsey terms into active and passive contributions. For the $\pi \leftrightarrow \pi$ term, we decomposed the active part further by specifying which of the two orbital groups, i.e., $\pi(\mathrm{C}_{2n})$ and $\pi(\mathrm{F})$, should be active or passive. Hence, the terms of Eqs. (1) and (2) are decomposed according to

$$J(\pi) = J(\pi)_a + J(\pi)_p, \tag{3a}$$

$$J(\pi(\mathrm{F})) = J(\pi(\mathrm{F}))_a + J(\pi(\mathrm{F}))_p, \tag{3b}$$

$$J(\pi(\mathrm{C}_{2n})) = J(\pi(\mathrm{C}_{2n}))_a + J(\pi(\mathrm{C}_{2n}))_p, \tag{3c}$$

$$J(\pi \leftrightarrow \pi) = J(\pi \leftrightarrow \pi)_a + J(\pi \leftrightarrow \pi)_p, \tag{3d}$$

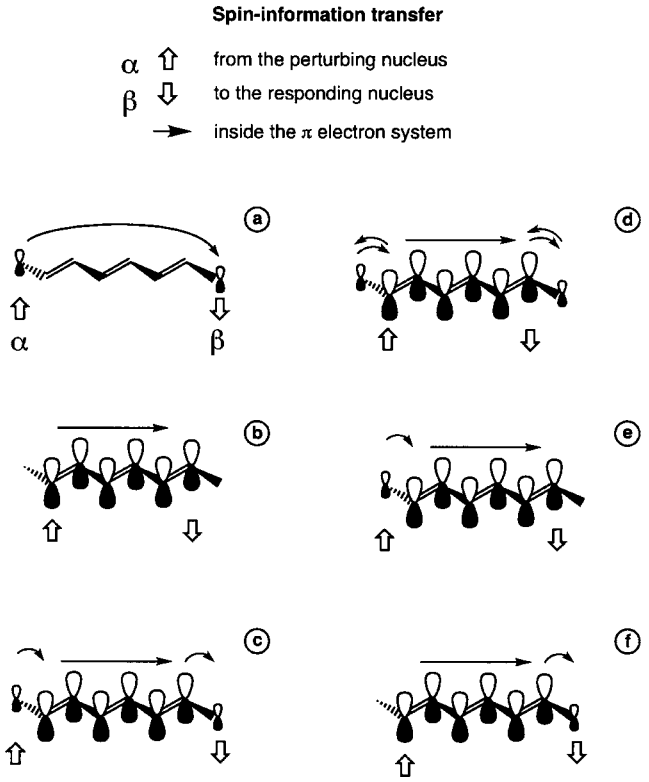

SCHEME 2. Spin-information transfer in a polyene via its π-orbitals. F^A is the perturbed, F^B is the responding nucleus. Contoured arrows indicate which of the π—orbitals receives the spin information from F^A or transmits it to F^B, respectively. Single arrows indicate spin-information transport within the π-orbital system. (a) From nucleus F^A via $\pi(F^A)$ directly to $\pi(F^B)$ and nucleus F^B. (b) From nucleus F^A directly to $\pi(C_{2n})$ and then to nucleus F^B. (c) From nucleus F^A via $\pi(F^A)$, $\pi(C_{2n})$ and $\pi(F^B)$ to nucleus F^B. (d) As in case (b), but with echo effects from $\pi(F^A)$ and/or $\pi(F^B)$. (e) From nucleus F^A via $\pi(F^A)$ and $\pi(C_{2n})$ to nucleus F^B. (f) From nucleus F^A via $\pi(C_{2n})$ and $\pi(F^B)$ to nucleus F^B.

$$J(\pi \leftrightarrow \pi)_a = J(\pi_a \leftrightarrow \pi_p) + J(\pi_p \leftrightarrow \pi_a) + J(\pi_a \leftrightarrow \pi_a). \tag{3e}$$

Here, $(\pi_a \leftrightarrow \pi_p)$ indicates that the π(F) system plays an active role whereas the $\pi(C_{2n})$ orbitals are purely passive, etc.

The active contributions defined in Eqs. (3a)–(3e) can, to a good approximation, be identified with individual orbital paths as shown in Scheme 2. For the $\pi(F)_a$ contribution, the spin information travels from the perturbing nucleus through the two π(F) orbitals to the responding nucleus, without any involvement from the $\pi(C_{2n})$ system [Scheme 2(a)]. The $\pi(C_{2n})_a$ contribution describes the process where the perturbing nucleus directly communicates spin information to the $\pi(C_{2n})$ system, which forwards it directly to the responding nucleus [Scheme 2(b)]. The $(\pi_p \leftrightarrow \pi_a)$ term describes a similar path as the $\pi(C_{2n})$ term, except that the π(F) orbitals make a passive contribution by a so-called echo effect[27] on the $\pi(C_{2n})$ system [Scheme 2(d)]. The $(\pi_a \leftrightarrow \pi_p)$ term reflects a spin-transport process, where the spin information propagates from the perturbing nucleus into the adjacent π(F) orbital, further through the $\pi(C_{2n})$ system, into the second π(F) orbital, and eventually to the responding nucleus [Scheme 2(c)]. Finally, the $(\pi_a \leftrightarrow \pi_a)$ summarizes the two equivalent paths shown in Schemes 2(e) and 2(f) where the orbital path involves the π(F) orbital at one of the coupling nuclei whereas the other nucleus communicates directly with the $\pi(C_{2n})$ system.

Local description of the coupling mechanism. The orbital analysis indicates which orbitals are most important for the transmission of the spin information. To understand the detailed coupling mechanism for these orbitals, graphical representations of local quantities are of great value.[26,32,35] The idea to describe NMR properties on a local basis goes back to Jameson and Buckingham;[36] Malkina and Malkin[37] and Soncini and Lazzeretti[38] have suggested alternative definitions of local densities for the description of indirect spin-spin coupling. In the present work, we will use the FC and SD magnetization densities[26,29,33] to compare the propagation of the spin polarization through the electron system for the FC and SD mechanisms.

III. COMPUTATIONAL DETAILS: CONVENTIONS

SSCCs were calculated at three levels of theory using (a) coupled perturbed density functional theory (CP-DFT) as described in Ref. 39 in connection with the B3LYP hybrid exchange-correlation functional;[40–42] (b) the SOPPA,[17,18] and (c) the complete-active-space self-consistent field (CASSCF) method for SSCC calculations.[43,44] Since the primary objective of this work is the analysis of the spin-spin coupling mechanism rather than the accurate reproduction of measured or the most reliable prediction of unknown SSCCs, SOPPA and CASSCF calculations were used for the only purpose of understanding shortcomings of the CP-DFT calculations and assessing the usefulness of the spin-spin coupling mechanism determined at the CP-DFT level of theory.

A $(15s7p2d/13s5pd/9sp)[15s6p2d/13s4pd/9sp]$ basis set was used for the calculation of the F,F-SSCCs. This basis set was derived from the $(11s7p2d/9s5pd/5sp)/[7s6p2d/5s4pd/3sp]$ basis set designed for NMR chemical shift calculations.[45,46] For the purpose of improving the latter basis set in the immediate vicinity of the nucleus (required to obtain reliable FC and SD terms[47,48]) the 1*s* basis functions were decontracted and four steep *s* functions were added whose exponents follow a geometric series with a progression factor of 6, starting with six times the exponent of the steepest primitive *s* function of the original basis set. The original $[7s6p2d/5s4pd/3sp]$ basis set was used for all other nuclei in the SSCC calculations.

The active space in the CASSCF calculations comprised the $\pi(C_{2n})$ orbitals and the π(F) orbitals, resulting in active spaces of the size (6,4), (8,6), (10,8), (12,10), and (14,12), respectively, for **1–5**.

For the HF wave functions of **1–5** used as the basis of the SOPPA calculations, stability tests[49] were performed. For comparison, the stabilities of the HF wave functions for **6–10** were determined at the same level of theory as for **1–5**.

Geometries were optimized at the B3LYP/6-31G(d,p) (Ref. 50) level of theory with the GAUSSIAN03 program package.[51] The analysis of the spin-spin coupling process was done with the COLOGNE07 package.[52] The SOPPA and CASSCF calculations were performed with the DALTON package.[53]

TABLE I. Ramsey terms of long-range *J* for the difluoropolyenes **1–5**, the polyenes **6–10**, and the modified difluoropolyenes **13–16**. All values given in hertz. Numbers in parentheses give contribution in question expressed in percentages with regard to the total SSCC. Only percentages above 5% are given. B3LYP calculations done using CP-DFT. All calculations done with a [15*s*6*p*2*d*/13*s*4*pd*/9*sp*] basis set ([7*s*6*p*2*d*/5*s*4*pd*/3*sp*] for noncoupling atoms). All geometries at B3LYP/6-31G(*d*,*p*).

Molecule	X,Y	Method	DSO		PSO		FC		SD		Total
1	$^{3}J(F^{A},F^{B})$	B3LYP	−1.70	(1.0)	−176.61	(98.4)	−30.41	(16.9)	29.17	(−16.2)	−179.56
		SOPPA	−1.71	(1.3)	−150.02	(110.8)	−9.36	(6.9)	25.72	(−19.0)	−135.37
		CASSCF	−1.69	(2.6)	−126.91	(192.0)	36.76	(−55.6)	25.76	(−39.0)	−66.09
		Expt.									−132.70[a]
		Expt.									−131.88[b]
		Expt.									−130.20···−133.79[c,d]
2	$^{5}J(F^{A},F^{B})$	B3LYP	−0.75	(−1.1)	24.13	(34.0)	7.27	(10.2)	40.38	(56.8)	71.03
		SOPPA	−0.76	(−1.4)	18.12	(32.5)	9.32	(16.7)	29.12	(52.2)	55.80
		CASSCF	−0.75	(−1.4)	13.10	(25.0)	17.60	(33.6)	22.45	(42.8)	52.40
3	$^{7}J(F^{A},F^{B})$	B3LYP	−0.40	(−1.7)	−4.89	(−20.5)	4.66	(19.5)	24.53	(102.7)	23.89
		SOPPA	−0.40	(−2.2)	−2.82	(−15.6)	5.31	(29.3)	16.09	(88.8)	18.12
		CASSCF	−0.40	(−2.2)	−1.48	(−8.2)	9.40	(52.1)	10.51	(58.3)	18.03
4	$^{9}J(F^{A},F^{B})$	B3LYP	−0.24	(−0.9)	1.15	(4.5)	3.69	(14.3)	21.13	(82.1)	25.74
		CASSCF	−0.24	(−1.5)	0.73	(4.4)	3.76	(22.7)	12.24	(74.0)	16.55
5	$^{11}J(F^{A},F^{B})$	B3LYP	−0.16	(−0.7)	−0.04	(−0.2)	3.12	(15.1)	17.71	(85.8)	20.65
		CASSCF	−0.16	(−1.8)	0.13	(1.5)	4.11	(46.2)	4.81	(54.1)	8.89
6	$^{3}J(H^{A},H^{B})$	B3LYP	−3.49	(−16.7)	2.79	(13.3)	21.33	(102.0)	0.28	(1.3)	20.92
7	$^{5}J(H^{A},H^{B})$	B3LYP	−1.31	(−71.2)	1.19	(64.4)	1.71	(92.8)	0.26	(14.0)	1.84
8	$^{7}J(H^{A},H^{B})$	B3LYP	−0.65	(−58.5)	0.57	(50.8)	1.01	(90.4)	0.19	(17.4)	1.12
9	$^{9}J(H^{A},H^{B})$	B3LYP	−0.38	(−43.0)	0.34	(38.0)	0.78	(87.4)	0.16	(17.7)	0.89
10	$^{11}J(H^{A},H^{B})$	B3LYP	−0.25	(−33.1)	0.22	(29.0)	0.65	(86.4)	0.13	(17.7)	0.76
13	$^{7}J(F^{C},F^{D})$	B3LYP	−0.37		−0.05		2.89	(19.9)	12.08	(83.0)	14.55
	$^{7}J(F^{A},F^{D})$	B3LYP	−0.31		0.56		3.19	(17.8)	14.53	(80.9)	17.97
	$^{7}J(F^{A},F^{B})$	B3LYP	−0.44		−3.51	(−21.1)	3.82	(23.0)	16.74	(100.8)	16.61
	$^{2}J(F^{A},F^{C})$	B3LYP	−0.89		−100.73	(89.1)	−22.05	(19.5)	10.59	(−9.4)	−113.09
14	$^{3}J(F^{A},F^{C})$	B3LYP	−0.05		−35.55	(116.8)	−30.80	(101.2)	35.95	(−118.1)	−30.44
	$^{6}J(F^{C},F^{B})$	B3LYP	−0.47		0.41		−17.27	(65.4)	−9.06	(34.3)	−26.39
	$^{7}J(F^{A},F^{B})$	B3LYP	−0.44		−5.31	(−28.2)	−0.64		25.23	(133.9)	18.84
15	$^{4}J(F^{A},F^{C})$	B3LYP	−0.91		2.34	(−6.2)	−23.79	(62.7)	−15.56	(41.0)	−37.92
	$^{5}J(F^{C},F^{B})$	B3LYP	−0.45		0.83		−0.05		23.89	(98.6)	24.23
	$^{7}J(F^{A},F^{B})$	B3LYP	−0.43		−4.36	(−18.6)	3.63	(15.5)	24.60	(104.9)	23.44
16	$^{7}J(F^{A},F^{B})$	B3LYP	−0.40		−5.51	(−10.8)	7.66	(15.1)	49.05	(96.5)	50.81

[a]Reference 19(a).
[b]Reference 19(b).
[c]Reference 19(c).
[d]Interval refers to different solvents, see Ref. 19(c).

All SSCC *J* values presented are related to the isotopes ^{1}H, ^{13}C, ^{19}F, and ^{35}Cl. Reduced SSCCs will be given in SI units of 10^{19} T^{2} J^{-2}. The molecules are placed in the *xy* plane in a way that the central C–C bond is parallel to the *y* axis. The coupling nuclei are denoted as *A* (perturbing) and *B* (responding), and the C atoms are numbered consecutively starting from the C atom bonded to the perturbing nucleus (see Scheme 1). The J-**OC**-PSP analyses were performed for localized molecular orbitals determined according to the Boys criterion.[54]

IV. CALCULATED SSCCs FOR FLUORINATED POLYENES

In Table I, calculated SSCCs $^{2n+1}J(F,F)$ for **1–5** and $^{2n+1}J(H,H)$ for **6–10** are listed together with their Ramsey terms. The SOPPA F,F-SSCCs are known to be rather reliable[16] as is reflected by the SOPPA value for **1** (135.4 Hz, Table I), which is just 3 Hz larger than the experimental value of 132±2 Hz. For **2–5** experimental F,F-SSCCs are not available; however, one can estimate for **2** a value close to 50 Hz (see below) again in reasonable agreement with the CASSCF and SOPPA values of Table I and results obtained

by Provasi *et al.*[16] We conclude that SOPPA values obtained in this and previous work provide reliable estimates of the F,F-SSCCs of the fluorinated polyenes under investigation. For **4**, the SOPPA calculation did not converge due to an external instability.

CASSCF values are largely parallel to SOPPA values (apart from **1**; see below) whereas CP-DFT/B3LYP F,F-SSCCs are too large by factors 1.4–2.5 (increasing from **1** to **5** compared to either SOPPA or CASSCF values). Inspection of the individual Ramsey terms shows, however, that the close agreement between CASSCF and SOPPA values is caused by a compensation of deviations. While the SD and PSO terms increase in the order CASSCF-SOPPA-B3LYP, the FC term (except for **1**) and PSO term increase in the order B3LYP-SOPPA-CASSCF.

The Ramsey terms in Table I give at hand that the exaggeration of the F,F-SSCCs in the B3LYP calculations is mainly caused by an overestimation of the SD term (except for **1**). Stability analyses[49] provide a clue to understand this overestimation. The Hartree-Fock (HF) wave functions for **1–5**, which are the basis for the SOPPA calculations, possess a triplet instability with a lowest eigenvalue of the Hessian of −0.0036 hartree (**1**) down to −0.0643 hartree (**4**). For **4**, there is a second negative eigenvalue of −0.013 hartree. The corresponding eigenvectors belong to triplet excitations within the $\pi(C_{2n})$ system, indicating that there are substantial nondynamical correlation effects within the $\pi(C_{2n})$ system. A comparison with the unsubstituted compounds **6–9** reveals the same qualitative behavior of the stability: all HF wave functions are externally unstable with lowest eigenvalues of −0.0006 hartree (**6**) to −0.0632 hartree (**9**) and a second negative eigenvalue of −0.0124 hartree for **9**. This finding corroborates that the observed instability is a property of the $\pi(C_{2n})$ system rather than caused by the F substitution. The triplet instabilities affect the calculation of the SD and FC terms. In the SOPPA calculations, electron correlation is treated explicitly, which reduces (but not eliminates) the impact of the instability on the FC and SD terms. The failure of the SOPPA calculation to converge for **4** indicates an insufficient description of the nondynamic correlation effects in the $\pi(C_{2n})$ system.

The CASSCF values for the F,F-SSCCs do not suffer from any instability of the wave function due to its multireference character, which includes nondynamic electron correlation thus avoiding an exaggerated magnetic response as at the B3LYP level. However, the good agreement of CASSCF with SOPPA values is fortuitous considering the fact that important dynamic correlation effects, accounted for by SOPPA, are not included into the CASSCF description. Such a fortuitous cancellation of different errors is no longer given in the case of **1** and leads to an underestimation of its F,F-SSCC by almost 70 Hz (Table I).

The B3LYP wave functions for **1–5** are stable, however, relatively close to a triplet instability. This near instability implies that the electronic response to the FC and SD perturbations tends to be exaggerated. This is in line with the overestimation of the SD term by B3LYP. The FC terms for **2–5** predicted by B3LYP are smaller than their SOPPA and CASSCF counterparts, which apparently is in contradiction to an overestimation of the magnetic response. However, one has to keep in mind that the FC mechanism is more sensitive to details of the orbitals (e.g., position of nodal surfaces and interference of different coupling paths) than the SD term, such that an exaggerated overall response not necessarily implies an overestimation of the FC term for an individual SSCC.

The PSO term is unaffected by triplet instabilities or near instabilities in the wave function. The observed deviations between B3LYP, SOPPA, and CASSCF values are mainly due to two causes: (i) missing dynamical correlation in the CASSCF wave functions and (ii) the fact that standard DFT does not describe exchange-correlation effects properly as soon as external magnetic fields give rise to orbital currents.[55]

Despite the obvious exaggeration of the absolute values of the F,F-SSCCs for **1–5** B3LYP predicts the right trends in total SSCCs and their Ramsey terms. In view of the fact that we focus in this work on a description of the spin-spin coupling mechanism rather than the prediction of accurate SSCCs, it is justified to carry out the analysis at the CP-DFT/B3LYP level of theory.

The calculated data in Table I reveal that $^{2n+1}J(F,F)$ as well as $^{2n+1}J(H,H)$ $(n=1,\ldots,5)$ decay slowly with increasing n where the long-range coupling is dominated by the FC (polyenes **6–10**) and SD mechanisms (fluorinated polyenes **1–5**). Apart from this, the $^{2n+1}J(F,F)$ values are substantially larger than the corresponding $^{2n+1}J(H,H)$ values, e.g., $^{11}J(F,F)$ in **5** is about 30 times as large as $^{11}J(H,H)$ in **10**. Considering that the gyromagnetic ratios of ^{19}F and ^{1}H are nearly equal, $\gamma(^{19}F)/\gamma(^{1}H)=1.062$ (25.1815 and 26.7522 $\times 10^7$ rad T^{-1} s^{-1}), the J values clearly indicate that the electronic coupling in **1–5** is much stronger than in **6–10**. The PSO contribution, although substantial for **1** and **2**, decays much more rapidly with n than the FC and SD contributions and plays no role for the long-range coupling in line with what was previously observed for polyenes **6–10**.[14] F,F spin-spin coupling in **1** is different from that found for **2–5** in that (a) the total SSCC is negative, dominated by a large negative PSO term, and (b) the SD term is smaller than for **2**. Obviously, the vicinal F,F coupling in **1** is dominated by short-range mechanisms that are not present in **2–5**. Therefore, **1** is excluded in the following when trends in $^{2n+1}J(F,F)$ values or its Ramsey terms for increasing n are analyzed and discussed.

V. ORBITAL DECOMPOSITION OF F,F COUPLING CONSTANTS

Table II presents the J-**OC**-PSP orbital decomposition of $J(F,F)$ for molecules **1–5**. Results reveal that the FC(π) and SD(π) terms decay *most slowly* with increasing n and thus *dominate* the long-range coupling in **1–5**. PSO(σ) and PSO(π) decay more rapidly, both at about the same rate, and FC(σ) and SD(σ) decay even more rapidly than the PSO contributions.

The long-range nature of the FC(π) and SD(π) coupling is a result of $\pi \rightarrow \pi^*$ excitations dominating these terms. For

TABLE II. J-**OC**-PSP analysis of $J(\mathrm{F},\mathrm{F})$ for the difluoropolyenes **1–5**. All values given in hertz. Calculations done with CP-DFT using the B3LYP functional and a [15*s*6*p*2*d*/13*s*4*pd*/9*sp*] basis set ([7*s*6*p*2*d*/5*s*4*pd*/3*sp*] for noncoupling atoms). Geometries at B3LYP/6-31G(*d*,*p*). Values in parentheses give the contribution in question expressed as percentage of the total SSCC, i.e., of the total B3LYP value given for the respective compound in Table I. Only percentages larger than 5% are given.

Molecule	A/P[a]	DSO	PSO		FC		SD		Total		Additivity[b]
σ											(1)
1		−1.62	−64.08	(35.7)	−41.93	(23.4)	11.39	(−6.3)	−96.24	(53.6)	
2		−0.68	8.50	(12.0)	1.19		3.01		12.02	(16.9)	
3		−0.35	−1.77	(−6.9)	0.12		−0.30		−2.30	(−9.7)	
4		−0.21	0.54		0.02		0.09		0.44	(−5.9)	
5		−0.14	0.02		0.00		−0.01		−0.13		
π total											(2)
1		−0.08	−112.53	(62.7)	11.52	(−6.4)	17.78	(−9.9)	−83.32	(46.4)	
2		−0.08	15.63	(22.0)	6.08	(8.6)	37.37	(52.6)	59.01	(83.1)	
3		−0.05	−3.12	(−12.1)	4.53	(17.6)	24.83	(96.5)	26.20	(109.7)	
4		−0.03	0.62		3.67	(15.4)	21.04	(88.1)	25.30	(105.9)	
5		−0.02	−0.07		3.12	(15.1)	17.73	(85.9)	20.77	(100.6)	
π(F)											(2.1)
1		0.10	−11.37	(6.3)	3.57		3.05		−4.66		
2		0.01	6.74	(9.5)	0.48		6.32	(8.9)	13.55	(19.1)	
3		0.00	−0.95		0.15		1.56	(6.1)	0.77		
4		0.00	0.23		0.07		0.89		1.18		
5		0.00	0.01		0.03		0.42		0.46		
$\pi(\mathrm{C}_{2n})$											(2.2)
1		−0.18	−61.29	(34.1)	2.63		−1.79		−60.63	(33.8)	
2		−0.09	3.13		2.18		7.13	(10.0)	12.34	(17.4)	
3		−0.05	−0.82		1.78	(6.9)	5.69	(22.1)	6.61	(25.7)	
4		−0.03	0.18		1.51	(6.3)	5.36	(22.4)	7.02	(29.4)	
5		−0.02	−0.02		1.32	(6.4)	4.79	(23.2)	6.06	(29.4)	
$\pi(\mathrm{F}) \leftrightarrow \pi(\mathrm{C}_{2n})$											(2.3)
1			−39.87	(22.2)	5.32		16.52	(−9.2)	−18.03	(10.0)	
2			5.77	(8.1)	3.42		23.92	(33.7)	33.11	(46.6)	
3			−1.36	(−5.3)	2.60	(10.1)	17.57	(68.3)	18.81	(73.1)	
4			0.20		2.09	(8.7)	14.80	(62.0)	17.10	(71.6)	
5			−0.05		1.77	(8.6)	12.53	(60.7)	14.24	(69.0)	
Detailed analysis for 3											
π(F)											
3	*a*	0.00	−0.94				1.57	(6.1)	0.63		(2.1.1)
3	*p*	0.00	−0.01		0.15		−0.01		0.14		(2.1.2)
$\pi(\mathrm{C}_{2n})$											
3	*a*	−0.05	−0.81				5.34	(20.7)	4.48	(17.4)	(2.2.1)
3	*p*	0.00	−0.01		1.78	(6.9)	0.36		2.13	(8.3)	(2.2.2)
$\pi(\mathrm{F}) \leftrightarrow \pi(\mathrm{C}_{2n})$											
3	*a*	0.00	−1.35	(−5.2)	0.00		17.66	(68.6)	16.31	(63.4)	(2.3.1)
3	*p*		0.00		2.60	(10.1)	−0.09		2.50	(9.7)	(2.3.2)
3	$a \leftrightarrow a$		−1.09				11.23	(43.6)	10.15	(39.4)	(2.3.1.1)
3	$a \leftrightarrow p$		−0.23				6.83	(26.5)	6.61	(25.7)	(2.3.1.2)
3	$p \leftrightarrow a$		−0.04				−0.40		−0.44		(2.3.1.3)

[a]Active/passive contribution. Rows without an entry in this column give total (active+passive) contributions.
[b]This column indicates how the individual J-**OC**-PSP contributions add upp: (2)=(2.1)+(2.2)+(2.3), (2.1)=(2.1.1)+(2.1.2), (2.2)=(2.2.1)+(2.2.2), (2.3)=(2.3.1)+(2.3.2), etc. The total SSCC is equal to (1)+(2).

the PSO term, these $\pi \rightarrow \pi^*$ excitations do not contribute due to the selection rules, which require a change in the magnetic quantum number by 1.[30] Accordingly, the PSO mechanism is dependent on excitations from π orbitals into less delocalized in-plane pseudo-π^* orbitals [for the PSO(π) terms] or from in-plane pseudo-π into π^* orbitals [for the PSO(σ) terms], which limits the range of the PSO coupling. The situation is different in polyynes, where both π_x and π_y orbitals are present, and $\pi_x \rightarrow \pi_y^*$ and $\pi_y \rightarrow \pi_x^*$ excitations make substantial contributions to the PSO coupling. This is in line

with the large PSO terms reported by Provasi *et al.*[16] for fluorinated polyynes. A remarkable feature of the PSO(σ) and PSO(π) contributions for **1–5** is that their sign alternates with increasing n, in distinction to the FC(π) and SD(π) terms, which are positive for all n values. This difference indicates the qualitative differences between the PSO coupling mechanism on the one hand and the FC and SD mechanisms on the other hand.

Given that the long-range coupling in **1–5** is provided by the FC(π) and SD(π) contributions, the following analysis will focus on these two terms.

F orbitals are known to possess long tails that might play an essential role in spin-spin coupling by establishing a through-tail mechanism as we described it for the vicinal H,H-SSCCs in ethane, which is dominated by the tail interactions of the CH bond orbitals.[11] Further decomposition of the FC(π) and SD(π) contributions reveals, however, that the term involving only π(F) orbitals decays rapidly with n (n=2: FC: 0.5 Hz, SD: 6.3 Hz, n=5: FC: 0.03 Hz, SD: 0.42 Hz; Table II). The delocalization of the π(F) orbitals is too weak to provide a long-range through-tail coupling[11,30] between the two F nuclei. Obviously, the $\pi(C_{2n})$ electron system and the $\pi \leftrightarrow \pi$ interaction terms are *essential* for the long-range SD and FC coupling. Both for FC and SD, these contributions decay slowly with increasing n. Actually, the decay for increasing n is somewhat slower for $\pi(C_{2n})$ (FC: value for n=5 is 60% of that for n=2, SD: 67%) than for $\pi \leftrightarrow \pi$ (FC: 51%, SD: 52%). For SD, the $\pi \leftrightarrow \pi$ terms are clearly dominating the $\pi(C_{2n})$ ones (ratio 3:1, Table II) whereas for the FC term the $\pi \leftrightarrow \pi$ and $\pi(C_{2n})$ contributions are comparable (ratio: 4:3, Table II). Actually, the $\pi \leftrightarrow \pi$ contribution to the SD term is the *largest* individual component of the total J(F,F), contributing over 60% of the total J(F,F) for $n=3\cdots5$ [$\pi(C_{2n})$ term: above 20%].

The $\pi(C_{2n})$ and the $\pi \leftrightarrow \pi$ contributions to the FC and SD terms decay monotonously and smoothly from **2** to **5**. This indicates that the corresponding coupling mechanisms are essentially the same throughout the series **2–5**. For the following more detailed investigations, we will therefore concentrate on molecule **3** rather than considering the complete series **2–5**. **3** can be considered as the smallest of the molecules **1–5** where the long-range coupling mechanism is fully established and no longer overlaid by short-range coupling mechanisms. This can be seen from the following facts: (i) The coupling is dominated by the FC and SD terms; the ratio of SD to FC terms is about constant (5:1 to 6:1). (ii) The FC and SD terms in turn are dominated by π contributions; the σ contributions amount to less than ±3% of the total FC or SD contributions. (iii) Among the π contributions, the π(F) term is small against the terms involving the $\pi(C_{2n})$ system. The ratio between the $\pi \leftrightarrow \pi$ and $\pi(C_{2n})$ terms is about constant (SD: about 3:1, FC: about 4:3).

The decomposition of the J-**OC**-PSP contributions for **3** into active and passive contributions is given at the end of Table II. For the FC term, the active part of all π contributions vanishes, in line with the discussion of the FC(π) mechanism in Sec. II. The SD term, in contrast, is dominated by active contributions. All passive contributions are negligible, their total contribution being 0.26 Hz or 1% of the total SSCC. This indicates that the SD π coupling mechanism is predominantly *active*, i.e., the π system interacts *directly* with the coupling nuclei. The $(\pi \leftrightarrow \pi)_a$ contribution in turn is dominated by the $(\pi_a \leftrightarrow \pi_a)$ part, which accounts for 11.2 Hz, or 44% of the total SSCC. Next important is the $(\pi_a \leftrightarrow \pi_p)$ term, which contributes 6.8 Hz or 26% of the total SSCC. The remaining terms make only small contributions.

TABLE III. Cartesian subcomponents for the SD(π) term in **3–5**, **11//3**, and **8//3**. All values given in hertz. Calculations done with CP-DFT using the B3LYP functional and a [15*s*6*p*2*d*/13*s*4*pd*/9*sp*] basis set ([7*s*6*p*2*d*/5*s*4*pd*/3*sp*] for noncoupling atoms). The geometry of **3** was optimized at the B3LYP/6-31G(*d*,*p*) level. Calculations for **11//3** and **8//3** performed at the geometry of **3**.

Molecule	Contribution	(*xx*)	(*yy*)	(*zz*)	(*xy*)	(*xz*)	(*yz*)
3	π total	13.35	12.26	51.21	0.12	−0.46	−0.83
	$\pi(C_{2n})$	3.22	2.61	11.62	0.14	−0.10	−0.22
	$\pi \leftrightarrow \pi$	9.21	8.73	35.89	−0.02	−0.22	−0.32
4	π total	8.52	12.49	41.65	0.00	0.02	0.21
5	π total	9.25	8.47	35.42	0.08	−0.01	−0.03
11//3	π total	−0.49	0.12	−0.67	−0.12	−0.012	0.002
8//3	π total	0.06	0.02	0.008	0.12	0.0004	0.0001

From the orbital decomposition, one can conclude that the orbital paths b, c, e, and f in Scheme 2 dominate the SD(π) coupling mechanism in **3**, where path b [corresponding to the $\pi(C_{2n})$ active contribution] contributes about 5.3 Hz, path c (corresponding to the $\pi_a \leftrightarrow \pi_p$ contribution about 6.8 Hz), and paths d and e (both entering with equal weight into the $\pi_a \leftrightarrow \pi_a$ contribution) about 11.2/2=5.6 Hz each. Accordingly, the four orbital paths b, c, e, and f in Scheme 2 contribute each between 5.3 and 6.8 Hz to the SD(π) coupling in **3**.

In Table III, the Cartesian subcomponents of the dominant SD contributions are listed. Analysis of these data confirms that the $\pi \rightarrow \pi^*$ excitations, which provide the long-range coupling mechanism, dominate the (*zz*) subcomponent and account for a substantial part of the (*xx*) and (*yy*) subcomponents, whereas they do not contribute to the remaining subcomponents.[32] The mechanistic analysis of the SD(π) contribution will thus focus at its (*zz*) subcomponent.

VI. ANALYSIS OF THE F,F SPIN-SPIN COUPLING MECHANISM

The (*zz*) subcomponents of the $\pi(C_{2n})$ and $\pi \leftrightarrow \pi$ contributions are responsible for the strong F,F coupling, where the SD(π) coupling predominantly derives from active contributions, i.e., the F nuclei interact directly with the π system.

For the purpose of analyzing how F substitution enhances the long-range coupling and especially the SD mechanism, we will compare **3** with two reference compounds, viz., hexatriene **8** and monofluorinated hexatriene **11**. For the calculations of both reference compounds, we use the optimized geometry of **3** such that spin polarization densities are directly comparable. To indicate this, the two ref-

TABLE IV. Ramsey terms of $^{7}K(X,Y)$ for **3**, **11//3**, **8//3**, **9**, **10**, and **12**. All K values given in SI units of 10^{19} T^2 J^{-1}, and J values given in hertz. Calculations done with CP-DFT using the B3LYP functional and a [15*s*6*p*2*d*/13*s*4*pd*/9*sp*] basis set ([7*s*6*p*2*d*/5*s*4*pd*/3*sp*] for noncoupling atoms). Geometries at B3LYP/6-31G(*d*,*p*).

						Total	
Molecule	X,Y	DSO	PSO	FC	SD	K	J
3	F, F	−0.04	−0.46	0.44	2.30	2.25	23.89
11//3	F, H	−0.04	−0.02	−0.20	−0.04	−0.25	−2.88
8//3	H, H	−0.04	0.03	0.13	0.01	0.13	1.56
8	H, H	−0.04	0.03	0.16	0.01	0.16	1.95
12	Cl, Cl	−0.02	−1.02	0.05	2.66	1.67	0.19
9	C1, C8	−0.03	0.06	1.49	2.41	3.94	2.99
10	C1, C8	−0.03	0.06	1.94	2.77	4.74	3.60
10	C2, C9	−0.02	0.02	1.67	0.40	2.08	1.58

erence compounds will be denoted as **8//3** and **11//3** in the following. In contrast, the notation **8** means compound **8** at its optimal geometry. In Table IV, the reduced SSCC and their Ramsey terms are given for **3**, **8//3**, **11//3**, and **8**. The geometry change from **8** and **8//3** decreases the FC term from 0.16 SI units to 0.13 SI units, whereas all other Ramsey terms remain unchanged up to 0.01 SI unit. This indicates that **8//3** is a reasonable model system for **8**.

A. Three-step model for the electronic long-range coupling

The long-range π electronic spin-spin coupling in polyenes can be decomposed into three parts: (1) polarization of the $\pi(C_{2n})$ system by the perturbing nucleus, either directly or by mediation of the $\pi(F^A)$ orbital; (2) spin-information transfer through the $\pi(C_{2n})$ subsystem; and (3) transfer of the spin information from the $\pi(C_{2n})$ system to the responding nucleus, either directly or involving the $\pi(F^B)$ orbital. Due to the reciprocity of spin-spin coupling, steps 1 and 3 will be equivalent if the two coupling nuclei are of the same species. The total value for the respective SSCC contribution can then be regarded as a product of three transmission factors, one for each step, which indicate how intense the coupling between the nuclei and the $\pi(C_{2n})$ system is (steps 1 and 3) or how the spin signal is attenuated along the $\pi(C_{2n})$ system (step 2). For long-range coupling (i.e., $n \geqslant 3$), one expects that the three steps are independent of each other, i.e., the transmission coefficient for step 2 should be independent of the type of the coupling nuclei (H or F) as should be the transmission coefficients for steps 1 and 3. This implies that the spin polarization profile in the $\pi(C_{2n})$ system should be approximately equal for **3** and **11//3** provided F is chosen as perturbing nucleus in the latter case. The FC and SD contributions to $^{m}K(F^A,Cm)$ $(m=1\cdots 2n)$ probe the spin polarization in the $\pi(C_{2n})$ system. Both for FC(π) and $SD_{(zz)}(\pi)$, the $^{m}K(F,C)$ contributions for **3** and **11//3** are nearly identical for $m \leqslant 5$ (see Table V). This confirms that steps 1 and 2 proceed in the same way in **3** and **11//3**, i.e., the spin transport within the $\pi(C_{2n})$ system is *largely independent* of a replacement of H by F at C6. Similarly, the coupling mechanism at the perturbing nucleus (step 1) is *independent* of the type of responding nucleus and vice versa (step 3).

TABLE V. Comparison of $^{m}K(F^A,Cm)$ $(m=1\cdots 2n)$ for **3** and **11//3**. All values given in SI units of 10^{19} T^2 J^{-1}. Calculations done with CP-DFT using the B3LYP functional and a [15*s*6*p*2*d*/13*s*4*pd*/9*sp*] basis set ([7*s*6*p*2*d*/5*s*4*pd*/3*sp*] for noncoupling atoms). Geometries at B3LYP/6-31G(*d*,*p*).

Molecule	$m=1$	2	3	4	5	6
FC(π)[a]						
3	−2.55	2.97	−1.70	1.53	−1.09	1.00
11//3	−2.55	2.96	−1.69	1.54	−1.05	1.13
SD(π)						
3	−6.61	5.29	−2.65	4.02	−1.26	2.86
11//3	−6.61	5.28	−2.63	4.00	−1.26	2.68
$SD_{(zz)}(\pi)$						
3	−11.96	11.63	−5.41	7.79	−2.51	5.76
11//3	−11.93	11.61	−5.39	7.74	−2.50	5.43

[a]FC(π) is the total FC term minus the FC term calculated with all π orbitals frozen, SD(π) analogously.

B. Analysis of the spin-dipole coupling mechanism

The orbital analysis has shown that the processes b, c, d, e, and f of Scheme 2 dominate the $SD_{(zz)}(\pi)$ contribution to F,F spin-spin coupling in **3**. Utilizing the three-step model, the four processes can be summarized as shown in Scheme 3: There are two different pathways for the spin information in step 1: the perturbing nucleus can polarize the $\pi(C_{2n})$ system either via its *s*- (σ-) orbitals or, more directly, via its π(F) orbital leading to contributions to SD(π) of 5.3+5.5 =10.8 Hz and 5.5+6.8=12.3 Hz, respectively. The same two pathways are found for step 3.

Investigation of the zeroth-order π(C1C2) orbital for **3** and **8//3** reveals that (a) the amplitude of π(C1C2) at and around the F nucleus in **3** is considerably larger than around the H nucleus in **8//3** and (b) the π(C1C2) orbital has a nodal surface between the F and C1 nuclei. This results from the fact that the F atom in **3**, in distinction to the coupling H atom in **11//3**, provides a low-lying occupied π orbital. The

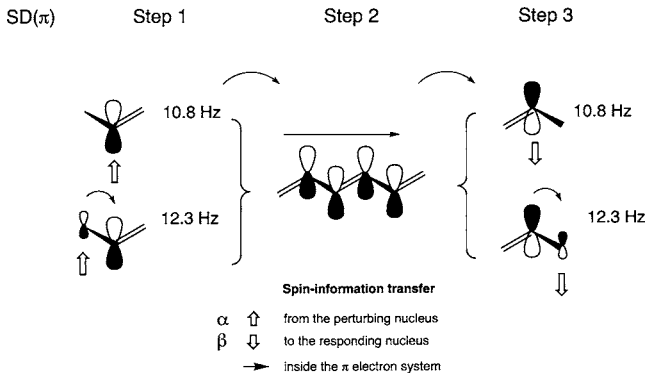

SCHEME 3. The three-step model for the electronic long-range coupling in compounds **1–5**. Step 1: Spin-polarization of the $\pi(C_{2n})$ system either directly or via the π lone-pair orbital of F^A. Step 2: Transport of the spin information through the $\pi(C_{2n})$ system. Step 3: Transport of the spin information to nucleus F^B either directly or via the π lone-pair orbital of F^B.

π(F) orbitals are lower in energy than the $\pi(C_{2n})$ orbitals and have no nodal surfaces. Consequently, the π(C5C6) orbital needs to have a nodal surface around the responding nucleus to maintain orthogonality between π(C5C6) and π(F) orbitals. We note that, as a common trait, all π orbitals show delocalization tails into neighboring π^* orbitals. These delocalization tails reflect the partial π character of the formal single C–C and C–F bonds and show that the π system forms one delocalized electron system, which is capable of long-range spin-information transfer.

In the case of **8//3**, the π(C1C2) orbital has no orthogonalization tail around the perturbing H nucleus, and its amplitude at the H nucleus is low. Neither is there a low-lying π^* orbital with a large amplitude at the perturbing H nucleus. Thus, the interaction between the H nuclear moment and the π-electron system is much weaker, resulting in a weak spin polarization of the $\pi(C_{2n})$ electron system.

The analysis of the $SD_{(zz)}(\pi)$ orbitals (which can be extended easily to a similar analysis of the SD spin densities) in **3** and **11//3** shows which features of **3** cooperate in providing a large electronic F,F coupling: (i) The presence of π and π^* orbitals at the coupling F nuclei provides an effective transfer of spin information into the electron system. The nuclear magnetic field overlaps strongly with the π and π^* orbitals, resulting in a large transition matrix element and allowing a large spin polarization without σ orbitals as intermediate links. (ii) The *strong* overlap and delocalization between π(F) and $\pi(C_{2n})$ system facilitates an efficient transport of the spin information within the π-electron system. An analysis of step 3, carried out in a similar way, shows that in the case of **11//3** the spin polarization of the $\pi(C_{2n})$ system is transferred to the responding H nucleus insufficiently thus causing a very weak SD coupling mechanism (Table IV).

C. Comparison between SD and FC terms

Each F substitution increases the $SD_{(zz)}(\pi)$ coupling by a factor of 80, whereas the corresponding increase for the FC(π) term is just by a factor of 2 (Table III). The main reason for this difference is the different role of σ orbitals for FC(π) and SD(π) coupling. In FC(π) coupling, σ orbitals around the coupling nuclei are essential to communicate the spin information between the coupling nuclei and the π-electron system. This means that F substitution does not imply a fundamental change in the FC(π) coupling mechanism: For a coupling H atom, the σ (CH) orbital connects the H nucleus with the $\pi(C_{2n})$ system. The σ(CH) orbital has a large amplitude at the H nucleus and is easy to polarize; thus, the FC(π) mechanism for H is relatively effective and dominates the long-range H,H coupling in unsubstituted polyenes (see Table III). By F substitution, the π-electron system is extended to the coupling nucleus; however, the additional π orbital still needs to communicate its spin information with the coupling nucleus by σ orbitals. Thus, F substitution does not change the coupling mechanism fundamentally. The σ(CF) orbitals in **8//3** and **3** have nodal planes close to the F nucleus and thus relatively small amplitudes at the site of the nucleus. Consequently, the F substitution results only in a moderate enhancement of the FC(π) coupling.

According to the selection rules for SD coupling,[32] σ orbitals cannot interact effectively with the coupling nuclei. The latter fact explains the small $SD_{(zz)}(\pi)$ coupling in **8//3**: The σ(CH) orbitals cannot mediate the spin information between the H nuclei and the $\pi(C_{2n})$ system in the same way as for the FC(π) coupling. F substitution provides a completely new situation: The π(F) orbital as well as the orthogonalization tails of the adjacent π(CC) orbitals, together with the $3p_z$(F) Rydberg orbital, provide a SD(π) coupling mechanism that is more effective than the FC mechanism because it does not require mediating σ orbitals. Thus, in **3**, the $SD_{(zz)}(\pi)$ mechanism outweighs the FC(π) mechanism for the long-range coupling.

So far, the focus has been on steps 1 and 3. As regards step 2, it was found in Sec. VI A that the spin-information transport through the $\pi(C_{2n})$ system is largely independent of F substitutions, i.e., proceeds in the same way for **8//3**, **11//3**, and **3**. The question arises whether there are nevertheless fine differences for FC(π) and SD(π) coupling mechanisms. For the purpose of answering this question, we have performed a correlation analysis between the π spin densities for the FC(π) and $SD_{(zz)}(\pi)$ contributions in **3** using as reference plane (size: 4.5×4.5 Å^2) the plane perpendicular to the molecule, containing C6 and F^B and being centered at the $C6F^B$ bond midpoint. This choice of the plane makes sure that differences in the spin densities due to step 1 do not influence the result. One finds actually a correlation coefficient of 0.999 99 between the two densities. This clearly indicates that the spin polarization in the $\pi(C_{2n})$ electron system proceeds in the *same* way for FC(π) and SD(π) coupling. The differences in the spin polarization profile caused in step 1 are decayed in the surrounding of the responding nucleus. Also, the π spin densities that convey the spin information to the responding nuclei in step 3 are identical (up to a factor), they are just probed differently by the responding nucleus. Obviously, the π-electron system is rather "rigid" and responds to quite different types of perturbations with similar spin polarization profiles. The latter is in line with our recent findings[14] that the π spin density in polyenes looks almost identical for different choices of the perturbing nucleus.

D. Comparison with other unsaturated molecules

The comparison of FC and SD mechanisms in **8//3**, **11//3**, and **3** indicates that in all cases where the coupling nuclei are connected by a contiguous π system, the SD term should be large and may even become the dominating contribution of the total SSCC. To test this conjecture, we calculated ^7K values for a number of polyenes and polyene derivatives, the results being summarized in Table IV. For dichlorohexatriene **12**, we find a FC value that is much smaller than in **3** (0.05 versus 0.44 SI units). The SD value, in contrast, is slightly larger for **12** than for **3** (2.7 versus 2.3 SI units). The comparison between **3** and **12** suggests that the SD term, in distinction to the FC term, in conjugated system is relatively insensitive to details of the molecule as long as the structure of the π system is maintained. This is plausible because the SD term, contrary to the FC term, does not de-

pend on details of the σ orbitals (position of nodal planes, etc.). For the $^7K(C,C)$ value in **9**, one finds a FC term of 1.9 SI units and a SD term of 2.4 SI units. The total K value for **9** is thus larger than that for **3** (3.9 versus 2.2 SI units). Even larger FC and SD terms (1.9 and 2.8 SI units, respectively) are obtained for $^7K(C1,C8)$ in **10**, with a total $^7K(C,C)$ value of 4.7 SI units. These examples suggest that a dominance of the SD term on the total SSCC, resulting in relatively large total SSCC values, should occur commonly for long-range SSCC in conjugated systems, in contradiction to the widespread belief that the SD term is generally negligible.

For all examples presented so far, the SD term was in the range of 2.3–2.7 SI units. This might suggest that the SD coupling of a given order in a conjugated system proceeds in a uniform fashion. However, the $^7K(C,C)$ values for **10** indicate that this is not generally true: $^7K(C1,C8)$ has FC and SD terms of 1.9 and 2.8 SI units, respectively. $^7K(C2,C9)$, in contrast, has a FC term of 1.7 SI units but a SD term of just 0.4 SI units, less than 20% of the corresponding terms for $^7K(C1,C8)$ in **10** or $^7K(F,F)$ in **3**. This appears surprising because just for $^7K(C2,C9)$ one has the same sequence of formal single and double bonds as for $^7K(F,F)$ in **3**. One has to keep in mind that the spin-information transport in a conjugated system is based on strongly delocalized occupied and virtual orbitals, which may imply both constructive and destructive interferences between individual contributions. Consequently, the absolute values of the SD contributions need not decay monotonously with increasing order n, and SD terms with equal n may differ markedly in their absolute value. For instance, the SD contribution to $^9K(C,C)$ in **10** is 2.0 SI units, i.e., exceeds its counterpart in $^7K(C2,C9)$ by a factor of 5.

The comparison with other conjugated systems has shown that **3–5** are not unique with regard to their long-range K values. This means that F,F couplings are not unique as regards large long-range electronic SD (π) coupling. However, the F atom is unique in that it combines two features, viz, (i) a large gyromagnetic ratio and (ii) a set of p valence electrons that can be incorporated in a π-electron system. The J values in Table IV demonstrate that the $^7J(F,F)$ value in **3** is by a factor of 6–10 larger than its counterparts for **9** and **10**, whereas **9** and **10** show larger ^7K values than $^7K(F,F)$ in **3**. Molecule **12** has a $^7SD(Cl,Cl)$ value larger than $^7SD(F,F)$ in **3** and $^7K(Cl,Cl)$ comparable to $^7K(F,F)$ in 3; however, the calculated $^7J(Cl,Cl)$ in **12** is less than 1% of $^7J(F,F)$ in **3**. Altogether, the coincidence of features (i) and (ii) makes F a good choice for the coupling nucleus.

VII. SUMMARY AND RELEVANCE OF RESULTS FOR QUANTUM COMPUTING

The investigation of the F,F coupling mechanism in molecules **1–5** makes it possible to answer the questions posed in the Introduction.

(1) The long-range F,F coupling in **1–5** is dominated by the SD(π) and, in second instance, FC(π) contributions. The PSO terms (both σ and π parts) decay more rapidly, and the SD(σ) and FC(σ) even more rapidly. The different decay of the SD(π) and FC(π) terms compared to PSO can be comprehended from the selection rules for the individual Ramsey terms: The excitations from (extended) π into (extended) π^* orbitals contribute to the FC and SD but not to the PSO term. The PSO term is dependent on excitations into (less extended) in-plane pseudo-π^* orbitals, which accounts for the more rapid decay. The selection rules[35] make it possible to comprehend the large PSO(π) terms predicted for polyynes and cumulenes:[16] Polyynes as well as cumulenes provide both π_y and π_z as well as π_y^* and π_z^* orbitals and therefore can undergo those excitations that are required for a large PSO current.[35]

(2) The through-tail interaction between the two π(F) orbitals decays more rapidly with the size of the molecule than the total $J(F,F)$ value. The large long-range coupling in **1–5** depends on the spin-information transfer through the $\pi(C_{2n})$ system rather than any through-tail interactions.

(3) F substitution in **1–5** influences the spin-information transfer between the nuclei and the electron system in two ways: (a) The π(F) orbitals provide a sensitive antenna for spin information. (b) The orbital-orthogonality requirements imply that the neighboring $\pi(C_{2n})$ orbitals obtain substantial delocalization tails at the F atoms. This improves the contact between the F nuclei and π-electron system. The impact of the extra π orbitals at the F atoms is different for the FC and SD terms.

   (a) *FC coupling mechanism*. FC(π) coupling always requires mediation by σ electrons between coupling nucleus and the π-electron system. Therefore, the additional contribution of the π orbitals at the F nuclei in **1–5** as compared to **6–10** is relatively small. In addition, different pathways for the σ mediation in **1–5** partly compensate each other in the total contribution.

   (b) *SD coupling mechanism*. As regards the SD term, the F nuclei interact with the π-electron system immediately. There is no effective mediation between nuclei and π electrons by the σ electrons. Thus, there is no effective long-range SD(π) coupling in **6–10**. In **1–5**, in contrast, the π(F) orbitals and the orthogonalization tails of the $\pi(C_{2n})$ orbitals provide two effective pathways for the spin information from the coupling nuclei into the $\pi(C_{2n})$ system and vice versa. Each of these pathways contributes similarly to the total SD coupling mechanism. Since no mediation by σ electrons is needed, SD coupling is more efficient than FC coupling.

(4) The spin-information transport inside the $\pi(C_{2n})$ system is not affected by the F substitution. The gain in efficiency arises from the improved contact between coupling nuclei and $\pi(C_{2n})$ system.

(5) The spin-information transport for the SD mechanism is nearly identical to that for the FC mechanism. This

gives further support to our previous findings[11,14] that the π-electron system has a very limited repertory of responses to external spin perturbations. The high efficiency of the SD coupling arises from the intense interaction between F nuclei and $\pi(C_{2n})$ electron system described in (2) rather than from a more efficient transmission of the spin information through the $\pi(C_{2n})$ system.

(6) The important feature of the F atom is a combination of two properties: (i) a large gyromagnetic ratio, which translates the efficient electronic coupling into a large J value, and (ii) the presence of π electrons that can be incorporated into a contiguous π system.

  (a) Being independent of mediating σ electrons and their particular features (nodal structure, etc.), the SD coupling mechanism through a π system is quite simple and insensitive to substitutions as long as the topology of the π-electron system is conserved. For instance, ^{7}SD(Cl,Cl) in **12** is just 10% larger than ^{7}SD(F,F) in **3**. This shows that the specific properties of F as small radius, high electronegativity, etc., are not crucial for a large electronic SD coupling.

(7) A corollary of (6) is that one can expect SD-dominated SSCC to occur commonly. If the coupling nuclei are connected by a contiguous π-electron system, it will be likely that the SD(π) system is more effective than the FC(π) mechanism for the reasons given in (2).

(8) Similarly as the SD(π) mechanism, the PSO(π) mechanism does not require mediation by σ orbitals. That is, in systems that allow for an efficient PSO(π) coupling, the PSO(π) term may dominate long-range coupling, and in analogy to (7), one may expect that long-range PSO(π)-dominated coupling is not restricted to a small class of systems but occurs commonly. According to the selection rules for the PSO term,[35] large PSO(π) coupling should be common in linear unsaturated molecules. This conjecture is supported by our previous findings.[35,56]

(9) Although the FC term is usually considered the dominating contribution to spin-spin coupling, findings of the current work emphasize that large long-range coupling is provided most efficiently by the SD and PSO terms. Given that a large PSO term requires a linear molecule (or a molecule with a linear moiety) and thus poses restrictions on the structure of the molecule, we predict that better possibilities to realize a large long-range coupling are given by the SD term.

(10) Long-range π spin-spin coupling is sensitive to the topology of the π system where this dependence deserves further attention.[57]

These findings provide guidance for the design of molecules that are suitable as active substances in NMR quantum computers. Synthesis of compounds **2–5** requires special means because fluorination normally leads to perfluorated compounds. The presence of another F atom in geminal or vicinal position to one of the coupling F nuclei leads to a significant reduction of the F,F-SSCC. For example, for 1,1,4,4-tetrafluorobutadiene the all-*trans* F,F-SSCC is reduced from ≈50 to 35.7 Hz.[15(a)] This trend is corroborated by calculated J(F,F) values for 1,1,6,6-tetrafluoro-all-*trans*-hexatriene **13** and 1,2,6-trifluoro-all-*trans*-1,3,5-hexatriene **14** (see Table I). For **13**, the ^7J(F,F) values are in the interval 14.6···16.6 Hz; for **14**, one gets a ^7J(F,F) value of 18.9 Hz, as compared to 23.9 Hz for **3**. In contrast, F substitution at C3 affects the ^7J(F,F) value only marginally: for 1,3,6-trifluoro-all-*trans*-1,3,5-hexatriene **15**, ^7J(F,F) is calculated to be 23.4 Hz, i.e., just 0.5 Hz lower than for **3**. Also, it is not useful to incorporate the polyene framework into a benzenoid hydrocarbon such as biphenyl, naphthalene, etc., because multipath coupling leads also to a reduction of the F,F-SSCC.[58]

The decrease of ^7J(F,F) in **14** as compared to **3** is in line with the general trend that electronegative substituents decrease long-range spin-spin coupling.[4] Conversely, electropositive substituents should result in an increase of J(F,F). This was tested by replacing the terminal H atoms in **3** by BH_2 groups, leading to compound **16**. Indeed, ^7J(F,F) for 16 was calculated as 50.8 Hz, more than twice the value for **3**. It is noteworthy that the variation of ^7J in **13–16** is dominated by variations in the SD term.

A substitution of the terminal H atoms in **3** by electropositive groups is interesting in another respect. It has been mentioned in Sec. I that active molecules for NMR quantum computing should contain active nuclei with different chemical shieldings.[9] The two F nuclei in **3** are equivalent and do not obey this requirement. By substituting just one of the terminal H atoms in **3** by an electropositive group, this equivalence is alleviated, and one obtains two nonequivalent nuclei while retaining the effective F,F spin-spin coupling observed in **3**. An alternative way to incorporate nonequivalent active nuclei in the molecule is pointed out by the results found for compound **15**: The F nucleus at C3 is nonequivalent to the terminal F nuclei, and the SSCCs between the nonterminal and the terminal F nuclei are 24.2 and −37.9 Hz, respectively, i.e., comparable to or larger than ^7J(F,F), respectively.

It remains to clarify how conformational flexibility of the polyenes discussed can lead to a change in the measured F,F-SSCCs. Previously,[14] we discussed this issue for the case of **7**, finding that the CCCC conformational angle in **7** is expected to fluctuate by no more than about ±10° and that the *cis* conformer of **7** is populated by just 0.7% at room temperature. Similar situations should hold for the other polyenes investigated. Hence, conformational flexibility should not have any sizable impact on the F,F-SSCCs. One could consider to suppress any conformational flexibility by incorporating the polyenes either into a liquid crystal or into a larger rigid molecule. However, in the former case, direct spin-spin coupling becomes relevant, whereas in the latter case, multipath coupling will decrease the F,F-SSCC values.

Altogether, it seems to be most prospective to focus on B-substituted derivatives of **2–5**, which of course have to be prepared by special synthetic methods.

ACKNOWLEDGMENTS

One of the authors (D.C.) thanks the University of the Pacific for support of this work. Calculations were done on the computers of the National Supercomputer Center (NSC) in Linköping. The authors thank the NSC and the Swedish National Allocations Committee for a generous allotment of computer time.

APPENDIX: J-OC-PSP ANALYSIS FOR FLUORINATED POLYENES

In this appendix we briefly outline the J-**OC**-PSP method and describe the detailed setup of the J-**OC**-PSP analysis for **1–5**.

The J-**OC**-PSP analysis is described in detail in Refs. 11, 14, and 29; here, we just summarize its main features. In a J-**OC**-PSP analysis, a SSCC under investigation is recalculated several times in a way that selected orbitals are *frozen*, i.e., their interaction both to the coupling nuclei and to the other orbitals is switched off, such that the frozen orbitals are kept fixed to the shape they have without the magnetic perturbation. By monitoring the change in the calculated SSCC occurring when an orbital or orbital group is switched from frozen to active status, one can infer the contribution of this orbital (group) to the total SSCC or its individual Ramsey terms. By combining appropriate frozen-orbital calculations, one can determine both contributions of individual orbital (groups) and contributions deriving from the cooperation of two or more orbital (groups). If the J-**OC**-PSP contributions are to be decomposed into an active and a passive part, the orbitals under investigation will not be switched from frozen to active state in one step but via an intermediate step, the *passive* state. For a passive orbital, the interaction with the coupling nuclei is switched off, whereas that with the other orbitals is maintained, so that the passive orbital can respond to changes in the remaining orbitals. If an orbital (group) is switched from frozen to passive, the change in the SSCC will provide the passive contribution of this orbital; if it is switched from passive to active, one gets the active contribution. The J-**OC**-PSP analysis can be performed for the total SSCC as well as for each of its Ramsey terms or for each Cartesian component or subcomponent, as applicable, of a Ramsey term.

We now describe the setup of the J-**OC**-PSP analysis of **1–5**. Selected-orbital calculations will be characterized by an expression of the form $[s_1 s_2]$, where s_1 describes the status of the π(F) orbitals and s_2 that of the $\pi(C_{2n})$ orbitals, according to s_1, $s_2 = a$ (active), p (passive), or f (frozen). The core and σ orbitals are active in all calculations. [That is, for instance, $[fp]$ describes a calculation where the π(F) orbitals are frozen and the $\pi(C_{2n})$ orbitals are passive, and all other orbitals are active. $[aa]$ describes a conventional SSCC calculation.] The J values obtained in selected-orbital calculations are then denoted by $J[\cdots]$. The individual J-**OC**-PSP contributions for **1–5** are calculated as follows:

$$J(\sigma) = J[ff], \tag{A1a}$$

$$J(\pi) = J[aa] - J[ff], \tag{A1b}$$

$$J(\pi(\mathrm{F})) = J[af] - J[ff], \tag{A1c}$$

$$J(\pi(C_{2n})) = J[fa] - J[ff], \tag{A1d}$$

$$\begin{aligned} J(\pi \leftrightarrow \pi) &= J(\pi) - J(\pi(\mathrm{F})) - J(\pi(C_{2n})) \\ &= J[aa] - J[af] - J[fa] + J[ff]. \end{aligned} \tag{A1e}$$

The decomposition into active and passive contributions is done according to the following equations:

$$J(\pi(\mathrm{F}))_a = J[af] - J[pf], \tag{A2a}$$

$$J(\pi(\mathrm{F}))_p = J[pf] - J[ff], \tag{A2b}$$

$$J(\pi(C_{2n}))_a = J[fa] - J[fp], \tag{A2c}$$

$$J(\pi(C_{2n}))_p = J[fp] - J[ff], \tag{A2d}$$

$$J(\pi)_p = J[pp] - J[ff], \tag{A2e}$$

$$J(\pi)_a = J(\pi) - J(\pi)_p = J[aa] - J[pp], \tag{A2f}$$

$$\begin{aligned} J(\pi \leftrightarrow \pi)_p &= J(\pi)_p - J(\pi(\mathrm{F}))_p - J(\pi(C_{2n}))_p \\ &= J[pp] - J[pf] - J[fp] + J[ff], \end{aligned} \tag{A2g}$$

$$\begin{aligned} J(\pi \leftrightarrow \pi)_a &= J(\pi \leftrightarrow \pi) - J(\pi \leftrightarrow \pi)_p \\ &= J[aa] - J[af] - J[fa] - J[pp] \\ &\quad - J[pf] + J[fp], \end{aligned} \tag{A2h}$$

$$J(\pi_a \leftrightarrow \pi_p) = J[ap] - J[af] - J[pp] + J[pf], \tag{A2i}$$

$$J(\pi_p \leftrightarrow \pi_a) = J[pa] - J[fa] - J[pp] + J[fp], \tag{A2j}$$

$$J(\pi_a \leftrightarrow \pi_a) = J[aa] - J[pa] - J[ap] + J[pp]. \tag{A2k}$$

[1] *Encyclopedia of Nuclear Magnetic Resonance*, edited by D. M. Grant and R. K. Harris (Wiley, Chichester, 1996), Vols. 1–8.
[2] J. A. Pople, W. G. Schneider, and H. J. Bernstein, *High-Resolution Nuclear Magnetic Resonance* (McGraw-Hill, New York, 1959).
[3] J. W. Emsley, J. Feeney, and L. H. Sutcliffe, *High Resolution Nuclear Magnetic Resonance Spectroscopy* (Pergamon, Oxford, 1966).
[4] H. O. Kalinowski, S. Berger, and S. Braun, ^{13}C-*NMR-Spektroskopie* (Thieme, New York, 1984) and references cited therein.
[5] H. Günther, *NMR Spectroscopy* (Thieme, New York, 1983).
[6] J. Stolze and D. Suter, *Quantum Computing: A Short Course From Theory to Experiment* (Wiley-VCH, Weinheim, 2004); M. Hirvensalo, *Quantum Computing* (Springer, Berlin, 2004).
[7] N. A. Gershenfeld and I. L. Chuang, Science **275**, 350 (1997); W. S. Warren, *ibid.* **277**, 1688 (1997); N. A. Gershenfeld and I. L. Chuang, *ibid.* **277**, 1689 (1997).
[8] R. Marx, A. F. Fahmy, J. M. Myers, W. Bermel, and S. J. Glaser, Phys. Rev. A **62**, 012310 (2000).
[9] R. C. Mawhinney and G. Schreckenbach, Magn. Reson. Chem. **42**, S88 (2004).
[10] M. Barfield, S. A. Conn, J. L. Marshall, and D. E. Miiller, J. Am. Chem. Soc. **98**, 6253 (1976).
[11] J. Gräfenstein and D. Cremer, Magn. Reson. Chem. **42**, S138 (2004).
[12] M. Barfield, *Encyclopedia of Nuclear Magnetic Resonance* (Ref. 1), p. 2520; B. Chakraborty and M. Barfield, Chem. Rev. (Washington, D.C.) **69**, 757 (1969).
[13] F. Bohlmann, C. Arndt, H. Bornowski, and K. M. Klein, Chem. Ber. **96**, 1485 (1963).
[14] J. Gräfenstein, T. Tuttle, and D. Cremer, Phys. Chem. Chem. Phys. **7**, 452 (2005).

[15] (a) K. L. Servis and J. D. Roberts, J. Am. Chem. Soc. **87**, 1339 (1965); (b) F.-J. Weigert and J. D. Roberts, *ibid.* **93**, 239 (1971); (c) Y. G. Gakh, A. A. Gakh, and A. M. Groenenborn, Magn. Reson. Chem. **38**, 551 (2000).
[16] P. F. Provasi, G. A. Aucar, and S. P. A. Sauer, J. Phys. Chem. A **108**, 5393 (2004).
[17] E. S. Nielsen, P. Jørgensen, and J. Oddershede, J. Chem. Phys. **73**, 6238 (1980); J. Oddershede, D. L. Yeager, and P. Jørgensen, Comput. Phys. Rep. **2**, 33 (1984).
[18] T. Enevoldsen, J. Oddershede, and S. P. A. Sauer, Theor. Chem. Acc. **100**, 275 (1998).
[19] (a) Y. Kanazawa, J. D. Baldeschwieler, and N. C. Craig, J. Mol. Spectrosc. **16**, 325 (1965); (b) G. J. den Otter and C. MacLean, Chem. Phys. **3**, 119 (1974); (c) A. M. Ihrig and S. L. Smith, J. Am. Chem. Soc. **94**, 34 (1972).
[20] N. Ramsey, Phys. Rev. **91**, 303 (1953).
[21] N. M. Peruchena, G. A. Aucar, and R. H. Contreras, J. Mol. Struct.: THEOCHEM **69**, 205 (1990).
[22] V. Barone, J. E. Peralta, and R. H. Contreras, J. Phys. Chem. A **106**, 5607 (2002); V. Barone, P. F. Provasi, J. E. Peralta, J. P. Snyder, S. P. A. Sauer, and R. H. Contreras, *ibid.* **107**, 4748 (2003).
[23] T. Tuttle, J. Gräfenstein, and D. Cremer, Chem. Phys. Lett. **394**, 5 (2004).
[24] O. L. Malkina, D. R. Salahub, and V. G. Malkin, J. Chem. Phys. **105**, 8793 (1996).
[25] W. D. Arnold, J. Mao, H. Sun, and E. Oldfield, J. Am. Chem. Soc. **122**, 12164 (2000).
[26] A. Wu, J. Gräfenstein, and D. Cremer, J. Phys. Chem. A **107**, 7043 (2003).
[27] J. Gräfenstein and D. Cremer, J. Chem. Phys. **120**, 9952 (2004).
[28] J. Gräfenstein and D. Cremer, J. Chem. Phys. **121**, 12217 (2004).
[29] D. Cremer and J. Gräfenstein, Phys. Chem. Chem. Phys. **9**, 2791 (2007).
[30] A. Wu and D. Cremer, Phys. Chem. Chem. Phys. **5**, 4541 (2003).
[31] L. D. Landau and E. M. Lifshitz, *Quantum Mechanics: Non-Relativistic Theory* (Pergamon, Oxford, 1977).
[32] J. Gräfenstein and D. Cremer, Chem. Phys. Lett. **387**, 415 (2004).
[33] H. Fukui, T. Tsuji, and K. Miura, J. Am. Chem. Soc. **103**, 3652 (1981); H. Fukui, K. Miura, K. Ohta, and T. Tsuji, J. Chem. Phys. **76**, 5169 (1982).
[34] A. R. Engelmann, R. H. Contreras, and J. C. Facelli, Theor. Chim. Acta **59**, 17 (1981); A. R. Engelmann, G. E. Scuseria, and R. H. Contreras, J. Magn. Reson. (1969-1992) **50**, 21 (1982).
[35] J. Gräfenstein and D. Cremer, Chem. Phys. Lett. **383**, 332 (2004); J. Gräfenstein, E. Kraka, and D. Cremer, J. Phys. Chem. A **108**, 4520 (2004).
[36] C. J. Jameson and A. D. Buckingham, J. Chem. Phys. **73**, 5684 (1980).
[37] O. L. Malkina and V. G. Malkin, Angew. Chem., Int. Ed. **42**, 4335 (2003).
[38] A. Soncini and P. Lazzeretti, J. Chem. Phys. **118**, 7165 (2003); **119**, 1343 (2003).
[39] V. Sychrovský, J. Gräfenstein, and D. Cremer, J. Chem. Phys. **113**, 3530 (2000).
[40] A. D. Becke, Phys. Rev. A **38**, 3098 (1988).
[41] C. Lee, W. Yang, and R. P. Parr, Phys. Rev. B **37**, 785 (1988).
[42] A. D. Becke, J. Chem. Phys. **98**, 5640 (1993); P. J. Stephens, F. J. Devlin, C. F. Chabalowski, and M. J. Frisch, J. Phys. Chem. **98**, 11623 (1994).
[43] R. Shepard, in *Ab Initio Methods in Quantum Chemistry*, Advances in Chemical Physics Vol. 69, edited by K. P. Lawley (Wiley-Interscience, Chichester, 1987), Pt. II, p. 63; B. O. Roos, in *Ab Initio Methods in Quantum Chemistry*, Advances in Chemical Physics Vol. 69, edited by K. P. Lawley (Wiley-Interscience, Chichester, 1987), Pt. II, p. 399.
[44] O. Vahtras, H. Ågren, P. Jørgensen, H. J. Aa. Jensen, S. B. Padkjær, and T. Helgaker, J. Chem. Phys. **96**, 6120 (1992).
[45] S. Huzinaga, Technical Report (University of Alberta, Edmonton AB, Canada, 1971).
[46] W. Kutzelnigg, U. Fleischer, and M. Schindler, in *NMR—Basic Principles and Progress* (Springer, Heidelberg, 1990), Vol. 23, p. 1; M. Schindler and W. Kutzelnigg, J. Chem. Phys. **76**, 1919 (1982).
[47] P. F. Provasi, G. A. Aucar, and S. P. A. Sauer, J. Chem. Phys. **112**, 6201 (2000).
[48] O. B. Lutnæs, T. A. Ruden, and T. Helgaker, Magn. Reson. Chem. **42**, S117 (2004).
[49] R. Seeger and J. A. Pople, J. Chem. Phys. **66**, 3045 (1977).
[50] P. C. Hariharan and J. A. Pople, Theor. Chim. Acta **28**, 213 (1973).
[51] M. J. Frisch, G. W. Trucks, H. B. Schlegel, G. E. Scuseria, M. A. Robb, J. R. Cheeseman, J. A. Montgomery, Jr., T. Vreven, K. N. Kudin, J. C. Burant, J. M. Millam, S. S. Iyengar, J. Tomasi, V. Barone, B. Mennucci, M. Cossi, G. Scalmani, N. Rega, G. A. Petersson, H. Nakatsuji, M. Hada, M. Ehara, K. Toyota, R. Fukuda, J. Hasegawa, M. Ishida, T. Nakajima, Y. Honda, O. Kitao, H. Nakai, M. Klene, X. Li, J. E. Knox, H. P. Hratchian, J. B. Cross, V. Bakken, C. Adamo, J. Jaramillo, R. Gomperts, R. E. Stratmann, O. Yazyev, A. J. Austin, R. Cammi, C. Pomelli, J. W. Ochterski, P. Y. Ayala, K. Morokuma, G. A. Voth, P. Salvador, J. J. Dannenberg, V. G. Zakrzewski, S. Dapprich, A. D. Daniels, M. C. Strain, O. Farkas, D. K. Malick, A. D. Rabuck, K. Raghavachari, J. B. Foresman, J. V. Ortiz, Q. Cui, A. G. Baboul, S. Clifford, J. Cioslowski, B. B. Stefanov, G. Liu, A. Liashenko, P. Piskorz, I. Komaromi, R. L. Martin, D. J. Fox, T. Keith, M. A. Al-Laham, C. Y. Peng, A. Nanayakkara, M. Challacombe, P. M. W. Gill, B. Johnson, W. Chen, M. W. Wong, C. Gonzalez, and J. A. Pople, GAUSSIAN 03, Revision B.05, Gaussian, Inc., Wallingford, CT, 2003.
[52] E. Kraka, J. Gräfenstein, M. Filatov, Y. He, J. Gauss, A. Wu, V. Polo, L. Olsson, Z. Konkoli, Z. He, and D. Cremer, COLOGNE 2007, University of the Pacific, Stockton, CA, 2007.
[53] C. Angeli, K. L. Bak, V. Bakken, O. Christiansen, R. Cimiraglia, S. Coriani, P. Dahle, E. K. Dalskov, T. Enevoldsen, B. Fernandez, C. Hättig, K. Hald, A. Halkier, H. Heiberg, T. Helgaker, H. Hettema, H. J. Aagaard Jensen, D. Jonsson, P. Jørgensen, S. Kirpekar, W. Klopper, R. Kobayashi, H. Koch, A. Ligabue, O. B. Lutnæs, K. V. Mikkelsen, P. Norman, J. Olsen, M. J. Packer, T. B. Pedersen, Z. Rinkevicius, E. Rudberg, T. A. Ruden, K. Ruud, P. Salek, A. Sanchez de Meras, T. Saue, S. P. A. Sauer, B. Schimmelpfennig, K. O. Sylvester-Hvid, P. R. Taylor, O. Vahtras, D. J. Wilson, and H. Ågren, DALTON, Release 2.0, 2005; see http://www.kjemi.uio.no/software/dalton/
[54] S. F. Boys, Rev. Mod. Phys. **32**, 296 (1960).
[55] A. K. Rajagopal and J. Callaway, Phys. Rev. B **7**, 1912 (1973).
[56] D. Cremer, E. Kraka, A. Wu, and W. Lüttke, ChemPhysChem **5**, 349 (2004).
[57] J. Gräfenstein and D. Cremer (unpublished).
[58] S. Berger, S. Braun, and H.-O. Kalinowski, *NMR-Spektroskopie von Nichtmetallen* (Thieme, New York, 1994), Vol. 4.